Physics Letters B 672 (2009) 6–11

Contents lists available at ScienceDirect

Physics Letters B

www.elsevier.com/locate/physletb

Single-proton removal reaction study of ^{16}B

J.-L. Lecouey [a], N.A. Orr [a,*], F.M. Marqués [a], N.L. Achouri [a], J.-C. Angélique [a], B.A. Brown [b], F. Carstoiu [a,c], W.N. Catford [d], N.M. Clarke [e], M. Freer [e], B.R. Fulton [f], S. Grévy [a,1], F. Hanappe [g], K.L. Jones [d,2], M. Labiche [a,3], R.C. Lemmon [d,4], A. Ninane [h], E. Sauvan [a,5], K.M. Spohr [i], L. Stuttgé [j]

[a] LPC-Caen, ENSICAEN, Université de Caen et IN2P3-CNRS, 14050 Caen Cedex, France
[b] NSCL, Michigan State University, East Lansing, MI 48824-1321, USA
[c] IFIN-HH, PO Box MG-6, 76900 Bucharest-Magurele, Romania
[d] Department of Physics, University of Surrey, Guildford GU2 7XH, UK
[e] School of Physics and Astronomy, University of Birmingham, Birmingham B15 2TT, UK
[f] Department of Physics, University of York, York YO10 5DD, UK
[g] PNTPM, CP-229, Université Libre de Bruxelles, B-1050 Brussels, Belgium
[h] Slashdev Integrated Systems Solutions, Rue de la Rochette, 26, B-5030 Gembloux, Belgium
[i] School of Engineering and Science, University of Paisley, Paisley PA1 2BE, Scotland, UK
[j] IPHC, Université Louis Pasteur et IN2P3-CNRS, 67037 Strasbourg Cedex 02, France

ARTICLE INFO

Article history:
Received 13 February 2008
Received in revised form 13 November 2008
Accepted 19 December 2008
Available online 31 December 2008
Editor: D.F. Geesaman

PACS:
27.20.+n
25.60.Gc
25.90.+k

ABSTRACT

The low-lying level structure of the unbound system ^{16}B has been investigated via single-proton removal from a 35 MeV/nucleon ^{17}C beam. The coincident detection of the beam velocity ^{15}B fragment and neutron allowed the relative energy of the in-flight decay of ^{16}B to be reconstructed. The resulting spectrum exhibited a narrow peak some 85 keV above threshold. It is argued that this feature most probably corresponds to a very narrow ($\Gamma \ll 100$ keV) resonance with a dominant $\pi(p_{3/2})^{-1} \otimes \nu(d^3_{5/2})_{J=3/2^+} + \pi(p_{3/2})^{-1} \otimes \nu(d^2_{5/2}, s_{1/2})_{J=3/2^+}$ configuration which decays by d-wave neutron emission.

Amongst the light exotic nuclei, the two-neutron halo systems are arguably the most intriguing. Apart from the halo character, these nuclei exhibit the so-called "Borromean" property whereby, in a three-body description, none of the constituent two-body subsystems — n–n and core–n — are bound [1]. Modelling such systems thus requires knowledge of the core–n interaction. Given that measurements of neutron scattering on the core nucleus are in practice impossible (except for ^{6}He and the α–n interaction), the interaction must be derived from the structure of the corresponding unbound nucleus — ^{10}Li, for example, in the case of ^{11}Li [2].

Currently the heaviest established two-neutron halo system is ^{17}B [3]. Analyses of both the ^{15}B fragment momentum distribution following the breakup of a ^{17}B beam [4] and the total reaction cross section on a carbon target [3] indicate that the halo neutrons wave function contains roughly equal admixtures of $\nu 1d^2_{5/2}$ and $\nu 2s^2_{1/2}$ configurations. The recent observation of the gamma-ray de-excitation of the two bound excited states of ^{15}B [5] in the dissociation of ^{17}B suggests that core excitations may also play a role [6,7].

Little, however, is known about ^{16}B. Its unbound nature was most recently confirmed by Kryger et al. in an investigation of the reaction products from the breakup of ^{17}C [8]. Evidence for a very low-lying state, some 40 keV above the ^{15}B–n threshold, together with indications for a higher lying level 2.40 MeV above threshold was found in a heavy-ion multi-nucleon transfer reaction study [9]. Whilst benefiting from the advantages of the high intensities of stable beams, such reactions suffer from very low cross sections, a complex reaction mechanism and hence selectivity, often coupled with significant backgrounds as illustrated by Ref. [9].

As originally demonstrated by the investigation of ^{10}Li by Zinser et al. [10], the few-nucleon breakup of high-energy radioactive beams can be employed to populate, and study through the fragment–neutron final-state interaction (FSI), unbound nuclei. In addition to benefiting from significant cross sections (typically 10–100's mb), the high energies result in the strong forward focussing of the reaction products (increasing the effective detection accep-

* Corresponding author.
E-mail address: orr@lpccaen.in2p3.fr (N.A. Orr).
[1] Present address: GANIL, Caen, France.
[2] Present address: Dept. of Physics and Astronomy, Rutgers University, NJ, USA.
[3] Present address: STFC Daresbury Laboratory, Warrington, UK.
[4] STFC Daresbury Laboratory, Warrington, UK.
[5] Present address: CPPM, Marseille, France.

0370-2693/$ – see front matter
doi:10.1016/j.physletb.2008.12.053

tances) and permit the use of very thick targets ($\sim$ 100's mg/cm^2). Consequently measurements with beam intensities as low as $\sim$ 100 pps are feasible. Importantly, as described by Zinser et al. within the context of the sudden approximation, the stripping at high energy of one or more protons (for example) will not, to a good approximation, perturb the configuration of the valence neutrons ($\Delta\ell_n \approx 0$). As such the choice of a projectile with a well-known structure should permit the structure of the final-states of the unbound system to be inferred.

The technique has been extended to proton-removal reactions at intermediate energies by Chen et al. [11]. Despite the weak binding of the valence neutron of the ^{11}Be projectile (S_n = 0.50 MeV) employed in their study, the "selection rule" argument ($\Delta\ell_n \approx 0$) based on the premise of the fast removal of the proton was shown to remain valid to a good approximation [11,12]. Specifically, the principal strength to a discrete state observed in the proton knockout to the ^{9}Li + n channel was s-wave, as would be expected given the dominant $\nu s_{1/2}$ ground-state configuration of ^{11}Be. In addition, an underlying "backgound" or non-resonant continuum, ascribed to a relaxation in the angular momentum selection rule arising from the reaction induced ^{9}Li fragment recoil, was required to describe the data.

A recent higher statistics investigation of the C(^{11}Be, ^{9}Li+n) reaction at 35 MeV/nucleon using a setup similar to that described here has allowed us to consolidate these conclusions [13,14]. Importantly, the angular acceptance for the neutron detection, and hence that for the reconstructed ^{9}Li + n relative energy, was much larger than in the work of Chen et al. [11,12]. As a result it could be firmly established that, beyond a broad continuum, the only well defined strength populated in the ^{9}Li + n system was s-wave [13,14], with no detectable yield to other states, such as the low-lying p-wave resonance [15]. That is to say, the discrete final-states populated via proton-removal correspond, to a good approximation, to those arising from the valence neutron configuration of the projectile. Despite exhibiting more limited statistics, these conclusions are further reinforced by the results obtained for two-proton removal from ^{11}Be, whereby the only significant strength observed in the ^{8}He + n system is s-wave [11–14].

In this spirit we report here on an investigation of the low-lying level structure of ^{16}B using single-proton removal from an intermediate-energy beam of ^{17}C. As discussed below, the shell structure of ^{17}C has been established by a number of recent experiments [16–21].

The ^{17}C beam of mean energy 35 MeV/nucleon was produced via the reaction on a Be target of a 63 MeV/nucleon ^{18}O primary beam supplied by the GANIL cyclotron facility. The beam velocity reaction products were analysed and purified using the LISE3 fragment separator [22]. The resulting secondary beam composition was 98% ^{17}C with an average beam intensity of $\sim$ 7000 pps. A time-of-flight measurement performed using the beam tracking detectors (see below) and a parallel-plate avalanche counter (PPAC) located some 24 m upstream of the secondary reaction target allowed the ^{17}C ions to be separated in the offline analysis from the remaining contaminants. The energy spread of the ^{17}C beam, as defined by the settings of the LISE spectrometer, was 2.5% ($\Delta E/E$). The effect on the relative energy between the fragment and neutron from the in-flight decay of an unbound system, such as ^{16}B, is negligible compared to the overall resolution (see below) and no event-by-event correction based on the measured beam energies was required.

The secondary beam was delivered using the separator onto a 95 mg/cm^2 ^{nat}C target. Owing to the relatively poor optical qualities of the secondary beam (beam spot size $\sim$ 10 mm diameter), two position-sensitive PPAC's located just upstream of the secondary reaction target and separated by 60 cm were used for tracking. The impact point of the beam on target was thus reconstructed event-by-event with a resolution of $\sim$ 1.5 mm (FWHM). The charged fragments from the reactions were detected and identified using a Si–Si–CsI telescope centred at 0° and located 11.3 cm downstream of the target. The two 500 μm thick silicon detectors, each comprising 16 resistive strips, were mounted such that the strips of the first detector provided for a measurement of position in the horizontal direction whilst those of the second detector the vertical position. The impact point along each strip was determined with a resolution of 1 mm (FWHM). In addition to the energy-loss measurements provided by the silicon detectors, the residual energy of each fragment was determined from the signals derived from the 5 × 5 cm^2, 2.5 cm thick CsI crystal. The measurement of the total energy deposited in the telescope was calibrated using a "cocktail" beam, which included ^{15}B, and for which the energy spread was 0.05%. Runs were made over a range of rigidity settings of the LISE spectrometer such that the ^{15}B calibration points covered the range of energies expected from the in-flight decay of ^{16}B. The total energy resolution of the telescope was determined to be 1.2% (FWHM). In addition to the measurements of breakup on the C target, data was also acquired with the target removed so as to ascertain the contribution arising from reactions in the telescope. As the reaction of interest — C(^{17}C, ^{15}B + n) — is a charge changing one, this contribution was found to be negligible as expected [23].

The neutrons were detected using 97 liquid scintillator elements of the DEMON array [24]. The modules, each of which has an intrinsic detection efficiency of $\sim$ 35% at 35 MeV, were arranged in a staggered two-wall type configuration covering polar angles up to 39° in the laboratory frame [25]. This arrangement provided for a reasonable detection efficiency for the ^{15}B + n reaction channel out to $\sim$ 5 MeV relative energy, whilst retaining a good resolution. The neutron energy was derived from the time of flight measured between the PPAC located closest to the target and DEMON. The final energy resolution was 5% (FWHM). The neutron energy spectrum exhibited, in addition to the beam velocity neutrons produced in the projectile breakup, a low-energy component arising from neutrons evaporated from the target. Such events were removed in the off-line analysis by imposing a low-energy threshold of 13 MeV [25].

The identification of the various boron isotopes in coincidence with fast neutrons ($E_n > 13$ MeV) is shown in Fig. 1 where two particle-identification parameters (PId) were reconstructed using the energy-losses from each of the two silicon detectors together with the residual energy derived from CsI crystals [25]. As may be seen, the ^{15}B fragments are clearly separated from the more prolific lighter mass isotopes. In addition, as expected, the neutrons detected in coincidence with the ^{15}B fragments exhibit energies centered around the ^{17}C beam energy per nucleon.

Turning to the results, the most easily extracted observable is the single-neutron angular distribution in coincidence with the ^{15}B fragments. As may be seen in Fig. 2, the angular distribution is very forward focussed, indicating that the in-flight decay is dominated by events with low relative energies. The angle integrated cross section is 6.5 ± 1.5 mb, in agreement with the value of 4.4 ± 0.3 mb obtained by Kryger et al. at a somewhat higher beam energy (52 MeV/nucleon) for the inclusive channel C(^{17}C, ^{15}B) [8].

The reconstructed ^{15}B–n relative-energy spectrum is displayed in Fig. 3. As expected, significant strength resides close to the decay threshold, in particular in the form of a very narrow structure (FWHM $\approx$ 100 keV) at $\sim$ 100 keV. It should be pointed out that the measured relative energy may be directly identified with the energy in ^{16}B provided that the ^{15}B fragment is in the ground state. As noted earlier, ^{15}B possesses two bound excited states (E_x = 1.33 and 2.73 MeV) [5]. Given the relatively limited yield (655 events) in the C(^{17}C, ^{15}B + n) channel, a triple coincidence measurement including gamma-ray detection was precluded. As discussed be-

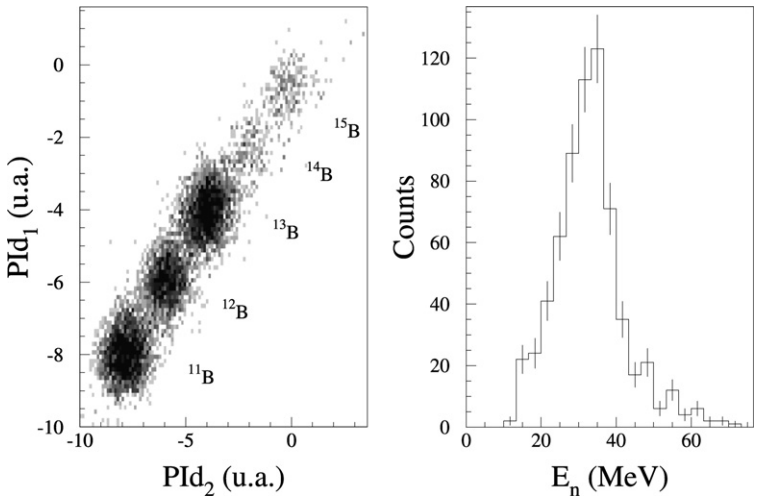

Fig. 1. Left panel: particle identification derived from the Si–Si–CsI detector telescope (see text) for the boron isotopes detected in coincidence with fast neutrons ($E_n >$ 13 MeV). Right panel: energy spectrum for neutrons detected in coincidence with ^{15}B fragments.

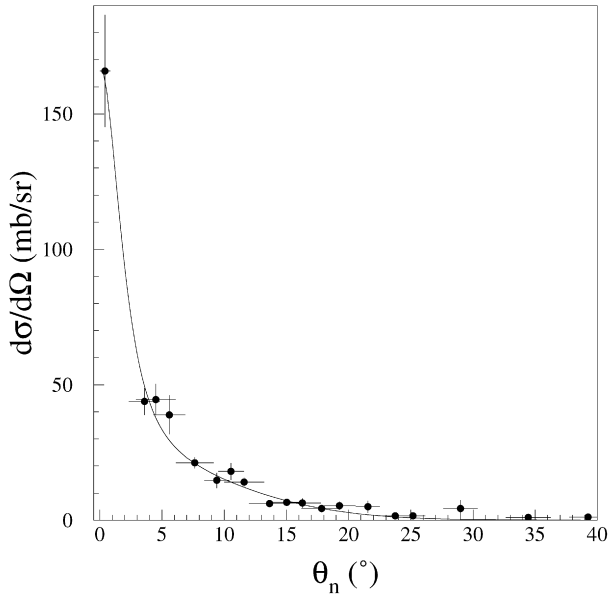

Fig. 2. Single-neutron angular distribution for the reaction C(^{17}C, ^{15}B + n) at 35 MeV/nucleon. The solid line is an adjustment to the data using a Lorentzian plus Gaussian lineshape [25].

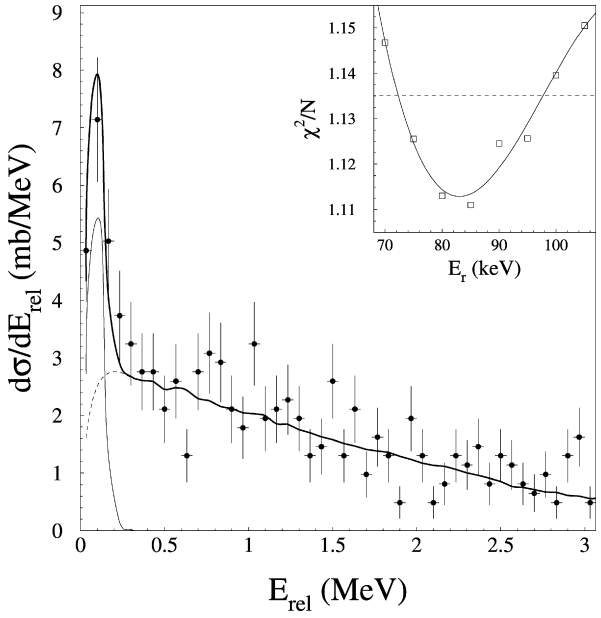

Fig. 3. Reconstructed ^{15}B–n relative energy spectrum. The thick solid line corresponds to the best adjustment to the data for a very narrow d-wave resonance ($E_r = 85 \pm 15$ keV, $\Gamma = 0.5$ keV) folded with the simulated experimental response function (thin solid line) plus a broad uncorrelated distribution obtained by event-mixing (dotted line) — see text. The insert shows the reduced χ^2 as a function of E_r, where the horizontal line delineates $\chi^2 + 1$.

low, the correspondence with the low-lying state observed by Kalpakchieva et al. [9] and structural considerations coupled to the relatively high energies of the bound excited states in ^{15}B suggest that the feature observed here does not arise from the decay of a high-lying level in ^{16}B to a bound excited state in ^{15}B.

Before proceeding any further in the interpretation, the effects of the experimental setup must be examined. The experimental response function was generated using a GEANT [26] based simulation code [25,27]. Owing to the granular character of the neutron-detection array, an important element in correctly determining the response function is the angular or transverse momentum distribution of the decaying ^{16}B system [25].

The transverse momentum distribution reconstructed from the measured momenta of the ^{15}B fragments and neutrons is displayed in Fig. 4. This observable provides further evidence supporting the approximate selection rule discussed above. More specifically, employing a "sudden approximation" type-calculation [28] based on the "black-disk" approach outlined by Hansen [29], the momentum distribution of ^{16}B produced via the removal of a well-bound ($S_p = 23$ MeV) $p_{3/2}$ proton from ^{17}C has been computed. The result, after inclusion of the various experimental effects, is displayed in Fig. 4 where the agreement is seen to be good. We note that a similarly good agreement with experiment has been obtained for ^{13}Be populated in single-proton removal from a 41 MeV/nucleon ^{14}B beam [25,30]. For the purposes of the calculation ^{16}B was treated as a barely bound system. This approximation and related uncertainties in the geometry of the projectile–target collision have a very limited influence on the form of the momentum distribution, which is essentially dictated by the angular momentum of the removed proton [28,29]. Indeed, as may be seen in Fig. 4, a more sophisticated calculation based on the eikonal approach [20], results in a transverse momentum distribution essentially identical to that of the simpler black-disk-type approach.

The predicted efficiency for detecting a ^{15}B–n pair is shown in Fig. 5. Importantly, the response is a smooth function of rel-

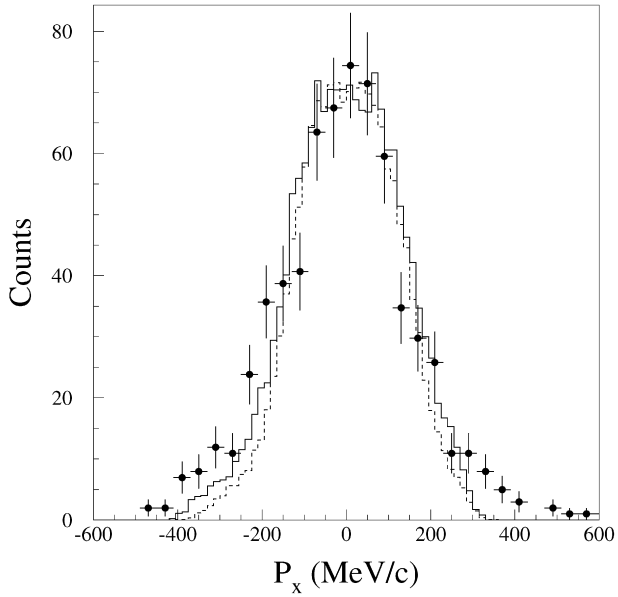

Fig. 4. Reconstructed ^{15}B–n transverse momentum distribution. The solid line is the result of a calculation (folded with the experimental effects and normalised to the peak number of counts) based on the sudden approximation for removal of a p-wave proton, bound by 23 MeV, from ^{17}C. An equivalent eikonal-type calculation is shown by the dashed line.

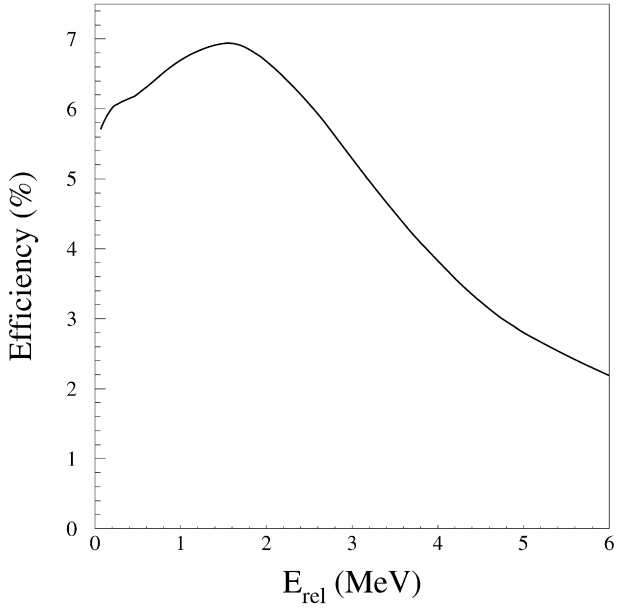

Fig. 5. Simulated detection efficiency for the ^{15}B–n pair as a function of relative energy (see text for details).

ative energy exhibiting no features which could mimic a sharp resonance-like state. The gradual fall off from a maximum of some 7% at around 1.5 MeV is in line with simple geometrical considerations based on the angular coverage of the neutron array (the efficiency for the detection of the ^{15}B fragments is essentially 100%). The resolution (FWHM) in the reconstructed relative energy, which is dominated by the finite angular size of the individual DEMON modules, was determined to vary as $0.320 \cdot \sqrt{E_{\rm rel}}$ (MeV), with a resolution of 100 keV at 100 keV decay energy. This suggests that the width of the feature observed in the decay spectrum (Fig. 3) is dominated by the experimental resolution. As a check on the simulations, comparison was made between the ^{7}He decay spectrum — the ground state resonance of which is well established — reconstructed from data acquired in the C(^{14}B, ^{6}He + n) reaction at 41 MeV/nucleon and that predicted by the Monte Carlo calculations. As discussed elsewhere the agreement was very good [25,30]. Cross-talk events, whereby scattering resulted in two detectors firing, were discarded by analysing only single-neutron events. The probability of cross-talk occurring was well reproduced by the simulations. Finally, we note that rate of events for which a neutron was first scattered without detection by a module (or non-active element in the setup) and then detected in another module was predicted to be less than $\sim 5\%$ of the total number of events and did not introduce noticeable distortions in the reconstructed relative energy spectrum.

In addition to the sharp resonance-like peak, the reconstructed ^{15}B–n relative-energy spectrum exhibits a very broad underlying distribution which slowly decays in intensity with increasing energy (Fig. 3). This distribution is interpreted as arising from the population of the non-resonant continuum via the ^{15}B recoil effect [11,12] and scattering of the ^{17}C valence neutron by the target.[6] Such events, for which no appreciable fragment–neutron FSI occurs, may be generated from the experimentally measured ^{15}B–n pairs via event mixing, a procedure which includes the effects of the experimental response function. In order to avoid the effects of possible residual correlations [31] an iterative technique was applied [32]. The uncorrelated distribution so generated and normalised to the data at high relative energy is shown in Fig. 3 (dashed line). The agreement is very good and reinforces the notion that the resonance-like peak is not an artifact of the experimental setup.

In order to interpret the data, the formalism developed in Refs. [10–12] has been followed. Briefly, the lineshape of the relative energy distribution is derived from the overlap of the initial bound-state wave function, describing the relative motion between the valence neutron and core of the projectile, and the unbound final-state wave function describing the fragment–neutron interaction. Here the wave functions were obtained using standard Woods–Saxon potentials ($r_0 = 1.25$ fm, $a_\nu = 0.6$ fm) adjusted to reproduce the neutron separation energy for the initial state and the resonance energy for the final state. As described in Refs. [25,33], for a narrow resonance ($\ell_n > 0$) this approach results in a lineshape essentially identical to a Breit–Wigner distribution incorporating the appropriate ℓ_n-dependent penetrability.

As discussed earlier, single-proton removal should, to a good approximation, leave the neutron configuration of the projectile unperturbed. The low-lying states populated in ^{16}B should, therefore, resemble a $\pi p_{3/2}$ hole coupled to the ^{17}C ground state neutron configuration. Shell model calculations indicate that the latter is dominated ($\sim 70\%$) by approximately equal admixtures of $\nu(d_{5/2})^3_{J=3/2^+}$ and $\nu(d^2_{5/2}s_{1/2})_{J=3/2^+}$ [17], as confirmed by recent measurements of neutron removal from ^{17}C [16,17,19,20]. As such a 0^-–3^- multiplet of states is expected to be preferentially populated in ^{16}B.

Calculations carried out here within the s–p–sd–fp model space using the WBP interaction [34] predict that such a low-lying multiplet is indeed present in ^{16}B (Fig. 6 and Table 1). The states which are expected to be populated will be $0\hbar\omega$ in character and may be identified by the spectroscopic factors for single-proton removal from the $\pi p_{3/2}$ orbital. As listed in Table 1, the first four levels predicted to be strongly populated are indeed the lowest lying 0^-–3^- states. Energetically the first three members of this multiplet can only neutron decay to the ^{15}B ground state (Fig. 6). Of the other states predicted to be strongly populated, only the 3^-_2

[6] Given the limited resolution and decreasing detection efficiency beyond $E_{\rm rel} \approx 2$ MeV (Fig. 5), a contribution arising from broad high-lying resonances cannot be discounted.

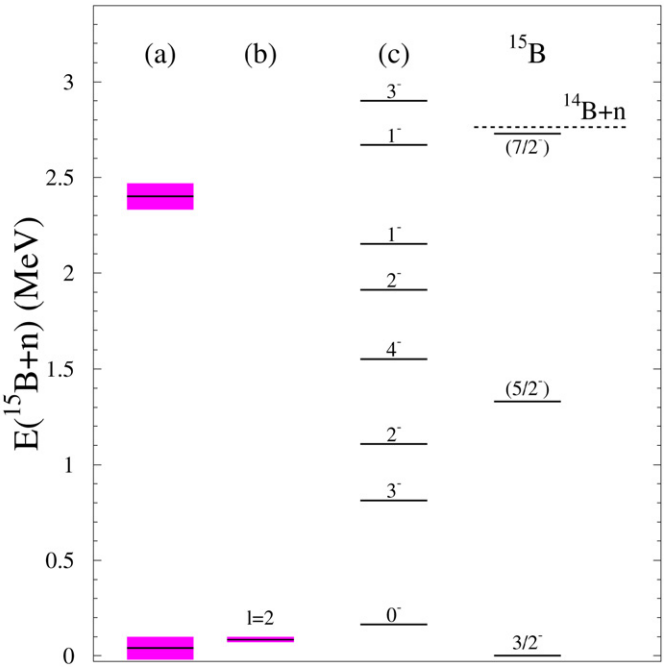

Fig. 6. Compilation of energy levels in ^{16}B measured in (a) the ^{14}C(^{14}C, ^{12}N)^{16}B reaction study [9], (b) the present work and (c) those predicted by $0\hbar\omega$ shell-model calculations to lie below 3 MeV (Table 1). The relative energy is given with respect to the neutron decay threshold. The shaded bands correspond to the uncertainties in the measurements. In the case of the shell model predictions, the energy of the ground state has been taken as the single-neutron separation energy of 164 keV predicted by Ref. [34]. The levels available for the neutron decay of ^{16}B to ^{15}B are also shown.

Table 1
Levels predicted to lie below 3.00 MeV in ^{16}B by $0\hbar\omega$ shell model calculations using the WBP interaction [34] in the s–p–sd–fp valence space. E_x is the excitation energy with respect to the 0^- ground state, which is calculated to lie 0.164 MeV above the ^{15}B–n threshold [34] ($E_x = E_r + 0.164$ MeV); C^2S is the spectroscopic factor for removing a $0p_{3/2}$ proton from ^{17}C; b_d is the spectroscopic factor for d-wave neutron decay to the ^{15}B ground state (these are only listed for states with non-zero C^2S) and σ_{-1p} is the cross section for proton-removal from ^{17}C estimated by an eikonal-type calculation and the corresponding spectroscopic factor (see text).

J^π	E_x (MeV)	C^2S	b_d	σ_{-1p} (mb)
0^-	0.0	0.27	0.08	2.6
3^-	0.649	1.10	0.37	10.5
2^-	0.943	0.32	0.65	3.0
4^-	1.389			
2^-	1.748	0.02	0.07	0.2
1^-	1.988	0.48	0.50	4.4
1^-	2.504			
3^-	2.736	0.45	0.28	4.0

($E_x = 2.736$ MeV) could, in principle, produce a narrow low-lying line in the relative energy spectrum via d-wave neutron decay to the second bound excited state of ^{15}B (Fig. 6). Such a scenario is, however, unlikely to be the origin of the peak observed here as only a small fraction of the decay is predicted to proceed in such a manner rather than to the ^{15}B ground state. In addition, the 3^-_2 may lie above the ^{14}B–n–n decay threshold, as predicted by the shell model calculations (Fig. 6). As such, it is reasonable to conclude that the peak observed in the ^{15}B–n relative-energy spectrum may be identified with one, or a combination, of the 0^-_1, 3^-_1 and 2^-_1 states.

The calculated spectroscopic factors for the neutron decay of the levels in ^{16}B to the ^{15}B ground state, which is the preferred decay channel, are listed in Table 1. All the states predicted to be strongly populated are, as simple considerations would suggest, expected to decay almost exclusively by d-wave neutron emission. The single-particle width for d-wave decay from a resonance at 100 keV is only 0.5 keV. Clearly then, the experimental resolution will dominate the lineshape of the low-lying states in the relative energy spectrum. Assuming a single, isolated low-lying resonance, described by an $\ell = 2$ Breit–Wigner lineshape modulated by the experimental response function, and the uncorrelated ^{15}B–n distribution described earlier, it was found that the reconstructed relative energy spectrum could be very well reproduced for a resonance energy $E_r = 85 \pm 15$ keV (Fig. 3). This is compatible with the lowest-lying feature observed in the multi-nucleon transfer reaction study of Kalpakchieva et al. [9] ($E_r = 40 \pm 40$ keV, $\Gamma < 100$ keV), supporting the contention that the peak observed here does not arise from the neutron-decay of a high lying-level in ^{16}B to a bound excited state in ^{15}B.

The detection of levels lying above ~ 2 MeV relative energy, such as the 1^-_2 and 3^-_2 states (Table 1) or the second peak observed by Kalpakchieva et al. [9] ($E_r = 2.32 \pm 0.07$ MeV), is challenging. As noted earlier, the resolution in the reconstructed relative energy grows poorer with increasing $E_{\rm rel}$ whilst the detection efficiency decreases monotonically from a maximum at around 2 MeV (Fig. 5). Simulations indicate that given the present statistics, the yields to levels with $E_{\rm rel} > 2$ MeV would need to be at least as strong as that observed to the low-lying peak to permit their identification.

The cross sections for nucleon removal or knockout reactions populating particle-stable states are commonly analysed within eikonal-type calculations (see, for example, Refs. [17,20,35] and references therein). Ideally, similar analyses might be employed to interpret experiments such as the present one populating particle unbound states. Difficulties, however, arise in such an approach owing to the need to approximate the composite unbound system as the core of the projectile. As such large uncertainties exist, most notably in the choice of the core–nucleon (here a proton) geometry and the core–target interaction. As noted above, the choice of these parameters has no significant influence on the shape of the momentum distributions, but unsurprising introduce large variations in the computed cross sections.

Bearing these limitations in mind, the cross sections to the states in ^{16}B below the ^{14}B–n–n decay threshold have been estimated within the eikonal approach using standard parameters [20] and the spectroscopic factors predicted by the shell model (Table 1). In terms of the yields, the most sensitive parameters are the radius and diffusivity of the Woods–Saxon potential describing the ^{16}B core–proton p-wave relative motion. Employing standard values of $r_0 = 1.25$ fm and $a_v = 0.6$ fm a summed cross section of some 24.7 mb (comprising the individual contributions listed in Table 1) was computed. Taking into account the reduction factor of ~ 0.3 observed in measurements of the removal a similarly strongly bound nucleon [35], a summed cross section of some 7.5 mb may be estimated. Whilst this is in good agreement with the yield observed here of 6.5 ± 1.5 mb, a number of caveats must be noted. First, a variation in r_0 of only 0.1 fm changes the calculated summed cross section by around 4 mb. Second, the reduction factors for strongly bound nucleon removal are relatively poorly established. Third, the yield in the observed ^{15}B–n relative energy spectrum arising from experimentally broadened states (see above) or those with relatively low yields cannot be determined. Thus, whilst the agreement between the predicted and measured cross section is encouraging it is premature to consider it as more than a guide and cannot be utilised to derive spectroscopic strengths.

In summary, the low-lying level structure of the unbound nucleus ^{16}B has been investigated via single-proton removal from a ^{17}C beam. The reconstructed ^{15}B–n relative energy spectrum exhibited a narrow resonance-like structure near threshold. Simple considerations, based on the premise of the fast removal of a $p_{3/2}$ pro-

ton from ^{17}C, and comparison with shell-model calculations suggest that this peak arises from a very narrow ($\Gamma \ll 100$ keV) resonance with a dominant $\pi(p_{3/2})^{-1} \otimes \nu(d^3_{5/2})_{J=3/2^+} + \pi(p_{3/2})^{-1} \otimes \nu(d^2_{5/2}, s_{1/2})_{J=3/2^+}$ configuration which decays by d-wave neutron emission.

Future measurements, with higher statistics and improved resolution may enable other states to be located and explore whether the peak observed here is a single-level. This is of some importance in the light of the shell model predictions of a number of states not observed here, as well as the apparent over estimation of the excitation energies of levels in neighbouring weakly-bound nuclei [5,36]. Whilst technically very challenging, the detection of gamma-rays in coincidence with the ^{15}B–n fragments should be included to remove any possible ambiguity regarding the excitation energies of the levels in ^{16}B. It is interesting to note that the preliminary analysis of a measurement undertaken at RIKEN of neutron removal from ^{17}B finds a ^{15}B–n relative energy spectrum almost identical to that reported here [37].

Finally, it is to be hoped that realistic reaction modelling of the population of unbound systems, which reaches beyond the simple considerations presented here and eikonal-type approaches (which treat the composite unbound system as a “core”), and can predicted the cross sections and lineshapes of the final-states will be forthcoming. In this context, the recent work of Blanchon et al. [38] is to be welcomed as a step in that direction.

Acknowledgements

The support provided by the technical staff of LPC and the LISE crew is gratefully acknowledged, as are the efforts of the GANIL cyclotron operations team for providing the primary beam. The assistance of S.M.G. Chappell, S.M. Singer, B. Benoit and L. Donadille in preparing various elements of the experiment is also acknowledged. Advice on aspects of the structure of light nuclei provided by D.J. Millener is appreciated. This work has been supported in part by the European Community within the FP6 contract EURONS RII3-CT-2004-06065 and, in the case of BAB, by NSF grant PHY-05553666.

References

[1] M.V. Zhukov, et al., Phys. Rep. 231 (1993) 151.
[2] I.J. Thompson, M.V. Zhukov, Phys. Rev. C 49 (1994) 1904.
[3] Y. Yamaguchi, et al., Phys. Rev. C 70 (2004) 054320, and references therein.
[4] T. Suzuki, et al., Phys. Rev. Lett. 89 (2002) 012501.
[5] M. Stanoiu, et al., Eur. Phys. J. A 22 (2004) 5.
[6] R. Kanungo, et al., Phys. Lett. B 608 (2005) 206.
[7] Y. Kondo, et al., Phys. Rev. C 71 (2002) 044611.
[8] R.A. Kryger, et al., Phys. Rev. C 53 (1996) 1971.
[9] R. Kalpakchieva, et al., Eur. Phys. J. A 7 (2000) 451.
[10] M. Zinser, et al., Phys. Rev. Lett. 75 (1995) 1719.
[11] L. Chen, et al., Phys. Lett. B 505 (2001) 21.
[12] L. Chen, PhD Thesis, Michigan State University (2000), http://www.nscl.msu.edu/ourlab/publications/download/Chen2000_28.pdf.
[13] H. Al Falou, Thesis, Université de Caen (2007), LPCC T 07-02, http://tel.archives-ouvertes.fr/docs/00/21/22/14/PDF/thesis.pdf.
[14] H. Al Falou, et al., in preparation.
[15] See, for example, H. Simon, et al., Nucl. Phys. A 794 (2007) 267;
H. Jeppesen, et al., Phys. Lett. B 642 (2006) 449, and references therein.
[16] E. Sauvan, et al., Phys. Lett. B 491 (2000) 1.
[17] V. Maddalena, et al., Phys. Rev. C 63 (2001) 024613.
[18] K. Ogawa, et al., Eur. Phys. J. A 13 (2002) 81.
[19] U. Datta Pramanik, et al., Phys. Lett. B 551 (2003) 63.
[20] E. Sauvan, et al., Phys. Rev. C 69 (2004) 044603.
[21] Z. Elekes, et al., Phys. Lett. B 614 (2005) 174.
[22] R. Anne, et al., Nucl. Instrum. Methods A 257 (1987) 215.
[23] F.M. Marqués, et al., Phys. Lett. B 381 (1996) 407.
[24] I. Tilquin, et al., Nucl. Instrum. Methods A 365 (1995) 446.
[25] J.-L. Lecouey, Thesis, Université de Caen (2002), LPCC T 02-03, http://tel.archives-ouvertes.fr/docs/00/04/54/66/PDF/tel-00003117.pdf.
[26] R. Brun et al., GEANT 3 user's guide, CERN/DD/EE/84.
[27] M. Labiche, Thesis, Université de Caen (1999), LPCC T 99-01;
M. Labiche, et al., Phys. Rev. Lett. 86 (2001) 600.
[28] F. Carstoiu, et al., Phys. Rev. C 70 (2004) 054602.
[29] P.G. Hansen, Phys. Rev. Lett. 77 (1996) 1016, and references therein.
[30] J.-L. Lecouey, et al., in preparation.
[31] W. Zajc, et al., Phys. Rev. C 29 (1984) 2173.
[32] F.M. Marqués, et al., Phys. Lett. B 476 (2000) 219.
[33] M. Thoennessen, et al., Phys. Rev. C 59 (1999) 111.
[34] E.K. Warburton, B.A. Brown, Phys. Rev. C 46 (1992) 923.
[35] A. Gade, et al., Phys. Rev. Lett. 93 (2004) 042501.
[36] M. Stanoiu, et al., Eur. Phys. J. A 20 (2004) 95;
D. Stohler, et al., Phys. Rev. C 77 (2008) 044303.
[37] T. Sugimoto, et al., RIKEN Accel. Prog. Rep. 37 (2004) 59;
T. Nakamura, private communication.
[38] G. Blanchon, et al., Nucl. Phys. A 784 (2007) 49.